

Contrast of LiFeAs with isostructural, isoelectronic, and non-superconducting MgFeGe

H. B. Rhee and W. E. Pickett

Department of Physics, University of California, Davis, CA 95616, USA

(Dated: August 22, 2012)

Stoichiometric LiFeAs at ambient pressure is an 18 K superconductor while isoelectronic MgFeGe is not, despite their extremely similar electronic structures. To investigate possible sources of this distinctively different superconducting behavior, we quantify the differences using first principles density functional theory, establishing first that the Fe total 3d occupations are identical in the two compounds. Individual 3d orbital occupations also differ very little (~ 0.01). The differences in Fermi surfaces (FSs) do not seem significant; however a redistribution of bands just above the Fermi level does represent a possibly significant distinction. Because the bands and FSs of LiFeAs are less in agreement with experiment than for other iron-pnictides, we study the effects of additional exchange-correlations effects beyond GGA (the generalized gradient approximation) by applying the modified Becke-Johnson potential (mBJ) exchange potential, which gives much improved bandgaps in insulators compared to GGA and might be useful for semimetals such as the Fe-based superconductors. Overall, we conclude that the mBJ corrections do not improve the description of LiFeAs as compared to experiment.

PACS numbers: 71.20.-b, 74.20.Pq, 74.70.Xa

I. INTRODUCTION

In the four years since the discovery of superconductivity in the iron-pnictide and -chalcogenide superconductors (FeSCs), a great deal has been learned about the materials physics of the handful of structural subclasses that comprise these new high temperature superconductors. Differences between the subclasses have been uncovered, but agreement on the microscopic mechanism of pairing is lacking. We suppose (as is commonly held) that the superconductivity that occurs in these materials which have in common a layered, fluorite-type Fe-Pn backbone (Pn = pnictide or chalcogenide) has a common origin, at least for the “high T_c ” (> 10 – 15 K) cases. One of the greatest current needs is to identify microscopic characteristics that can shed light specifically on the existence, or not, of high temperature superconductivity (HTS) and thereby on the underlying pairing mechanism.

Several mechanisms have been put forward. Because superconductivity borders and competes with magnetic order as in the HTS cuprates, it is natural to study a spin fluctuation (SF) origin, and several groups^{1–4} have pursued antiferromagnetic SF models. A *ferromagnetic* SF model has been suggested by Brydon *et al.*,⁵ largely on the basis on the poor nesting of its calculated FSs. Fe 3d orbital occupation and character have received much attention, and an orbital fluctuation (OF) model has been suggested by Saito *et al.*⁶ The role of the Pn anion was given more attention in the charge fluctuation (CF) picture of Zhou *et al.*,⁷ where interatomic Fe-Pn charge-charge interactions provided another elec-

tronic mechanism. On one hand, the mixing of the narrow Fe 3d bands removes almost all Pn character in the states near the Fermi level ε_F , making most models focus simply on the 3d states. On the other hand, T_c has been found to correlate strongly with the distance of the Pn above and below the Fe plane, or more specifically on the Pn-Fe-Pn bond angle and/or Fe-Pn bond length.

The Pn anion received attention early in the study of FeSCs, when Berciu *et al.*⁸ modeled pairing in terms of electronic polarons and bipolarons. Their picture foreshadowed the CF model mentioned above, but placed more emphasis on the anticipated large polarizability of the Pn anions, and did not include consideration of SFs or OFs. This picture was continued and extended to include interatomic exchange coupling by Chan *et al.*⁹ The conventional phonon mechanism, for which there is a reliable microscopic theory when electronic interactions are described sufficiently by density functional methods, has been evaluated by Boeri *et al.*¹⁰ and found to be too weak to explain T_c in the 25–55 K range. Strong spin-lattice coupling, however, has been suggested by Egami *et al.*¹¹ to be involved in pairing. The electronic structure of these FeSCs is being studied in detail experimentally and modeled carefully by numerous groups, with a primary aim being to identify the pairing mechanism.

LiFeAs is recognized as a problem child in the categorization of FeSCs. Among the vast collection of FeSCs that have been discovered since the first of their kind,¹² LiFeAs is one of very few which superconduct without the need for either chemical doping or physical compression. Of these few, LiFeAs

not only has the highest superconducting transition temperature ($T_c = 18$ K), but it is to date the only compound, other than LiFeP, whose T_c does not increase when doped or pressurized. It is widely believed that in the majority of FeSCs, doping or application of pressure suppresses the nesting-induced spin-density-wave order to make way for competing superconductivity. LiFeAs however does not undergo any magnetic transition, and significance of FS nesting in LiFeAs has been questioned.¹³ Not only does LiFeAs not fit well with many aspects of FeSCs, its behavior also differs strongly from its isovalent sister compound NaFeAs. Similarities between NaFeAs and LiFeAs in band structure and density of states are even more profound^{14,15} than between MgFeGe and LiFeAs, but unlike MgFeGe and LiFeAs, NaFeAs undergoes a magnetically driven structural phase transition above the superconducting transition.^{16–18} In fact, bulk superconductivity may not even exist in NaFeAs.^{19–21}

The recent report of the synthesis and characterization by Hosono’s group²² of non-magnetic MgFeGe, which is isostructural and isoelectronic with the 18 K superconductor LiFeAs but is not superconducting, provides a means to obtain new insight. In their initial report, Liu *et al.*²² noted the resemblance of the electronic structure near ε_F to that of LiFeAs, providing both a conundrum and an opportunity to identify differences that account for the vast distinction in superconducting behavior. Supposing that Mg gives up both of its valence electrons to the Fe-Ge bands, two initial basic questions emerge: the 3d charge on Fe, and the distinctions between the anions As and Ge that are neighbors in the periodic table. We first establish that the Fe 3d occupation is identical in these two compounds. The (presumably) more highly charged Ge anion should have an even higher polarizability than As, for which the simplest viewpoint might suggest to be more *favorable* for superconductivity, rather than precluding it. Moreover, the As-Fe-As angle, which has been shown for most of the pnictides^{23,24} to correlate strongly with increased T_c as it approaches the regular tetrahedral angle of 109.47° , is 103.1° , very similar to MgFeGe’s Ge-Fe-Ge angle of 103.6° . (Note that NaFeAs, which possesses an angle of 108.3° , is a departure from these two compounds in this respect.) One can also wonder whether the alkali/alkali earth atom can make any real difference. Otherwise, the essential difference would come down to small differences on the Fe atom, such as individual orbital occupations, which, as we show, are quite small.

In this paper we perform a close comparison of the electronic structures of MgFeGe and LiFeAs. The differences of the Fe 3d orbital occupations are

small but clear. Because the local density approximation (LDA) and generalized gradient approximation (GGA) have deficiencies in their description of the magnetism and atomic structure of these FeSCs, generally and LiFeAs in particular, we assess the effect of using the modified Becke-Johnson (mBJ) form of exchange-correlation potential²⁵ that builds in “exact exchange” in a local-density manner. The mBJ potential has now been established to provide excellent bandgaps in many semiconductors and insulators. Although it is not clear from most band structures, the FeSCs are close to a semimetallic state. Lebègue *et al.*²⁶, in their Fig. 15, show that in the as yet unsynthesized LaOFeN the occupied and unoccupied bands form disjoint complexes. This observation raises the question whether these same exact-exchange corrections might apply to a semimetal.

II. ELECTRONIC STRUCTURE

A. Description of methods

The non-magnetic electronic structures of LiFeAs and MgFeGe were calculated using WIEN2K,^{27,28} a density functional theory (DFT)-based full potential, linearized augmented planewave (LAPW) code. For the exchange-correlation functional, the generalized gradient approximation (GGA) of Perdew, Burke, and Ernzerhof²⁹ was applied. A k -point mesh of $32 \times 32 \times 19$ was used, and RK_{max} was set to 10. As for the muffin-tin (MT) radii R , we used values of 2.50, 2.43, and 2.14 a.u. for Li/Mg, Fe, and As/Ge, respectively. We adopted the experimental lattice constants of LiFeAs and MgFeGe (both of which form a $P4/nmm$ tetragonal unit cell) given in Refs. 22 and 30 respectively. The internal coordinates came from the same experiments, and relaxation was not applied in our calculations since we are interested in identifying distinctions and comparing with experiment when possible. The structural parameters are given in Table I. Note that the Li (Mg) atom is five-coordinate with As (respectively, Ge) in a square-based pyramid, and its height above the Fe plane is 2.20 Å (2.13 Å).

B. Bands and densities of states

The densities of states (DOSs) of LiFeAs and MgFeGe are displayed in Fig. 1. In the case of LiFeAs, the Fermi energy ε_F sits on the shoulder of a high DOS region with almost entirely Fe d character, consistent with results presented by Singh,³¹ Nekrasov *et al.*,³² and Liu *et al.*²² Li/Mg contribu-

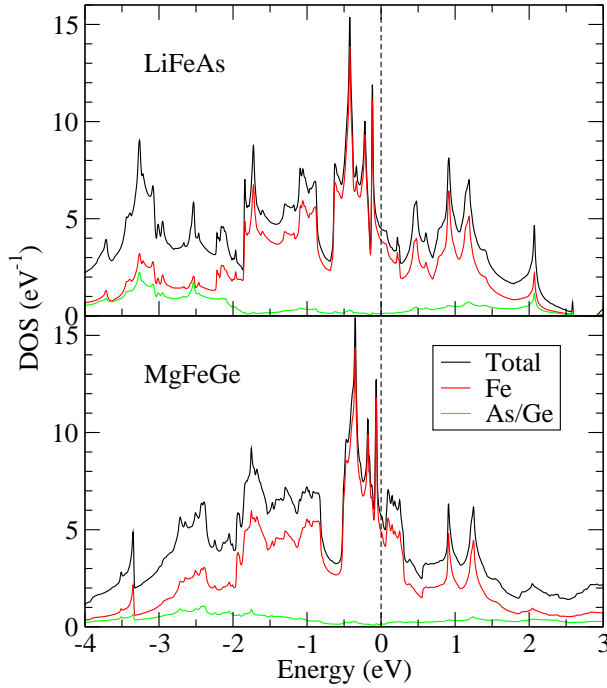


FIG. 1: (Color online) Densities of states (per two spins, per primitive cell) of LiFeAs and MgFeGe. Li/Mg states give negligible contribution in this energy range so they have not been plotted. The primary difference occurs in the 0.0–0.5 eV regions (see text).

tions are negligible at and around the Fermi energy, and As/Ge density is also very low at ε_F . The large DOS at ε_F , $N(\varepsilon_F)$, is a distinctive feature of LiFeAs compared to the smaller values in the other iron-pnictides, and MgFeGe shares this large value. In fact, $N(\varepsilon_F)$ is 25% larger in MgFeGe than in LiFeAs, a property that should *enhance* superconductivity independent of mechanism rather than hinder it. While a set of experimental data has been used to characterize LiFeAs as intrinsically overdoped³³ to explain its 18 K critical temperature, from its larger $N(\varepsilon_F)$ value due to ε_F falling further below the val-

TABLE I: Crystal structure parameters of LiFeAs and MgFeGe in the tetragonal space group $P4/nmm$. Wyck-off labels of Li/Mg, Fe, and As/Ge are, respectively, 2c, 2b, and 2c.

	a (Å)	c (Å)		(x, y, z)
LiFeAs	3.7914	6.3639	Li	(1/4, 1/4, 0.8459)
			Fe	(3/4, 1/4, 1/2)
			As	(1/4, 1/4, 0.2635)
MgFeGe	3.8848	6.4247	Mg	(1/4, 1/4, 0.8316)
			Fe	(3/4, 1/4, 1/2)
			Ge	(1/4, 1/4, 0.2620)

ley in the DOS it would seem to be underdoped.

The LiFeAs and MgFeGe DOSs share similar Fe d features from -2 eV up to ε_F , at which point, in MgFeGe, the shoulder is more abruptly cut off. The subband DOS peak of unoccupied states centered at 0.5 eV in LiFeAs is shifted down in MgFeGe, to form a denser manifold just above the abridged shoulder, and is centered 0.2 eV above the Fermi level. The separation of the Fe DOS into orbital components will be given later, when effects of different exchange-correlation functionals are discussed.

The band structures of the compounds are compared in Fig. 4. As noted by Liu *et al.*, the similarity of their bands near ε_F is the most striking feature. The doubly degenerate band at Γ drops by less than 0.1 eV to lie exactly at the Fermi level in MgFeGe, and the pocket at M shrinks in size due to a rise by less than 0.1 eV of the band just below ε_F ; the bands elsewhere at ε_F are extremely similar. The increased concentration of states in MgFeGe just above the Fermi level, visible in the DOS as mentioned above, can be traced to the lowering by 0.38 eV (from 0.43 eV to 0.05 eV) of the lowest unoccupied band at the X point. The FSs of LiFeAs and MgFeGe, discussed in more detail in later sections and shown in Fig. 7 and Fig. 8, are each made up of three hole pockets centered at Γ and two electron pockets at M. The electron FSs and the largest hole pocket increase in size in MgFeGe, while the two smaller electron pockets shrink. We have verified that changes due to spin-orbit coupling are uninterestingly tiny.

C. Charge density differences

The Fe 3d occupations in LiFeAs and MgFeGe are identical. This essential feature is established by comparing the radial valence charge density $r^2\rho(r)$ of Fe between the two compounds, shown in Fig. 3. In the region of the 3d peak at radius $r = 0.7$ a.u., where the density is due only to 3d occupation and to identical core tails, the difference is incredibly small (less than 0.1%), and the difference remains tiny out to 1.4 a.u. Using the same MT radius of 2.43 a.u., the charge of Fe in this neighborhood in LiFeAs is larger only by 0.01 electrons, with this tiny difference arising from the differing As and Ge tail charges. The orbital occupation matrix elements $n_{mm'}$ for both compounds are listed for comparison in Table II. No difference is larger than 0.015, which is the change for the d_{z^2} ($m = 0$) orbital, being smaller in MgFeGe. This difference is compensated by the $d_{xz/yz}$ occupations ($m = \pm 1$) increase by ~ 0.01 in MgFeGe. The $m = \pm 2$ (d_{xy} , $d_{x^2-y^2}$) orbital occupation changes are negligible. The t_{2g} and

e_g degeneracies are broken by the Fe site symmetry, of course, as can be noted in the occupation matrices.

D. As- and Ge-related differences

Since the total Fe 3d occupation and even individual orbital occupations differ little between the two compounds, it becomes of more interest to compare differences ascribable to As and Ge. One difference is the structure itself: the lattice constants a and c of MgFeGe are about 2.5% and 1% larger respectively. Of Fe's three nearest-neighbor interatomic distances, the Fe-Fe distance changes most, from 2.68 Å to 2.75 Å, the 2.5% increase directly related to the same relative increase in a lattice constant. Effective d - d hopping amplitudes might be changed somewhat, however, since the hopping is largely through the As or Ge atom and this interaction will differ. There is a similar 2% increase in the Fe-As/Ge distance (2.42 Å/2.47 Å), related to Ge's slightly larger atomic radius. Despite MgFeGe's larger unit cell (6% in volume), and Mg having larger nuclear charge than Li, but perhaps because Mg has an additional valence electron, the Fe-Mg distance is 0.8% *shorter* than that of Fe-Li (2.91 Å versus 2.88 Å).

The Pn-Fe-Pn angles have been observed to correlate very strongly with the maximum value of T_c observed within a structural class while varying stoichiometry and also across structural classes.^{23,24} This correlation does not extend well to the Fe chalcogenides, however, so its relevance in this comparison of LiFeAs to MgFeGe may be questioned. The similarity of the angles for these two compounds seems to make the bond angle a non-issue in the question of presence or absence of superconductivity.

There has been interest in the polarizability of the pnictide atom and its effect on carriers. The polarizability of the Ge atom is 40% larger than that of As (6.07 vs. 4.31, in 10^{-24} cm³). Naively, this difference would favor superconductivity in MgFeGe according to the relevant model.³⁴ Moreover, with the additional valence electron (Mg vs. Li) not going to Fe and thus going primarily to Ge, this difference in polarizabilities of Ge and As may be enhanced in the solid, making it even more difficult to understand the difference in superconducting behavior.

E. Susceptibility $\chi_0(\mathbf{q})$

In Fig. 2, we show the calculated constant-matrix-element bare susceptibilities $\chi_0(\mathbf{q})$ (normalized by $\chi_0(\mathbf{q} = 0)$) of LiFeAs and MgFeGe, accounting for

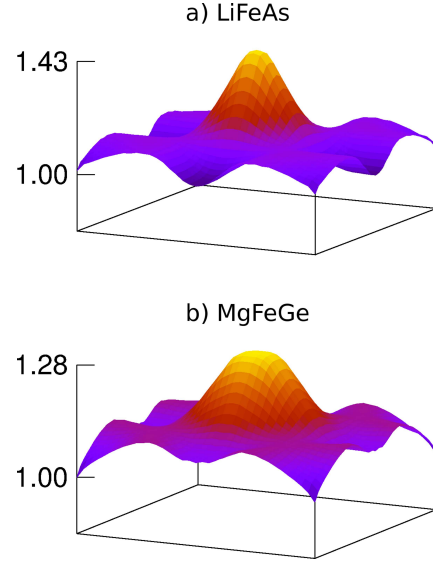


FIG. 2: (Color online) Non-interacting spin susceptibilities $\chi_0(q_x, q_y, q_z \equiv 0)$, each normalized by the χ_0 value at $\mathbf{q} = (0, 0, 0)$, of (a) LiFeAs and (b) MgFeGe in the complete Brillouin zone. In these plots, the Γ point is positioned at the corners.

all bands that cross the Fermi level. Our susceptibility for LiFeAs is consistent with that of Lee *et al.*,³⁵ who also observe a maximum in χ_0 at (π, π) . The two Γ -centered cylindrical FSs with radii $k_{F,1}$, $k_{F,2}$ (see figures below) lead to the circular hump in the range of $2k_{F,1}$, $2k_{F,2}$, and $k_{F,1} + k_{F,2}$. Small differences in the band structure broaden the (π, π) peak in MgFeGe, but the overall χ_0 topology is similar to that of LiFeAs. Applying dynamical mean field theory (DMFT) to DFT, in which dynamical electron correlation effects are taken into account, Lee *et al.* demonstrate a significant suppression in the strength of the peak and suggest this change is significant for its superconductivity (but to complicate things, several experimental groups^{36–39} have reported the existence, of varying degrees, of antiferromagnetic fluctuations). Application of DMFT to MgFeGe could be very instructive in trying to understand differences underlying the different superconducting behavior of these two very similar compounds.

III. APPLYING THE MODIFIED BECKE-JOHNSON POTENTIAL

Whereas the observed FSs in several iron-pnictides agree rather well with first principles results, the agreement has been worse for LiFeAs. Not only effective masses, but also sizes of the FSs are

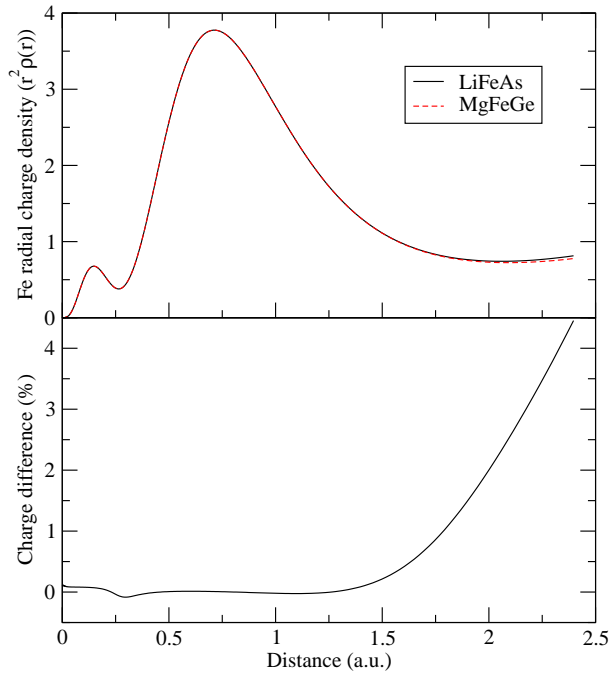


FIG. 3: (Color online) Valence radial charge density (in a.u.) of Fe in LiFeAs and MgFeGe (top), illustrating the extreme similarity not only in the region of the 3d peak at 0.7 a.u., but also extending out to 1.4 a.u. The tiny difference is quantified by plotting the percentage difference (bottom). Both are plotted versus the radial distance from the Fe atom center.

renormalized substantially from calculated results. LiFeAs is however a good non-magnetic Fermi liquid and the effects of interactions as obtained within DMFT treatments do not show much more than these changes (such as strong satellites, for example). Thus a mean field treatment of the electronic structure can be fairly accurate, but it is not the one given by the GGA functional. For this reason we have investigated the changes given by a recent extension of density functional exchange-correlation functionals.

We have applied the mBJ exchange potential, in the form known as the TB-mBJ potential (after Tran and Blaha's²⁵ modification), to both LiFeAs and MgFeGe. The mBJ potential is an extension of the Becke-Johnson potential,⁴⁰ which itself was formulated to reproduce the shape of the atomic optimized effective potential,^{41,42} an exact exchange potential. This goal is approached in a phenomenological manner through the use of orbital kinetic energy densities expressed in local-density form. The mBJ potential produces rather accurate gaps for a wide range of semiconductors and insulators, but as a local density functional it is much more cost-effective

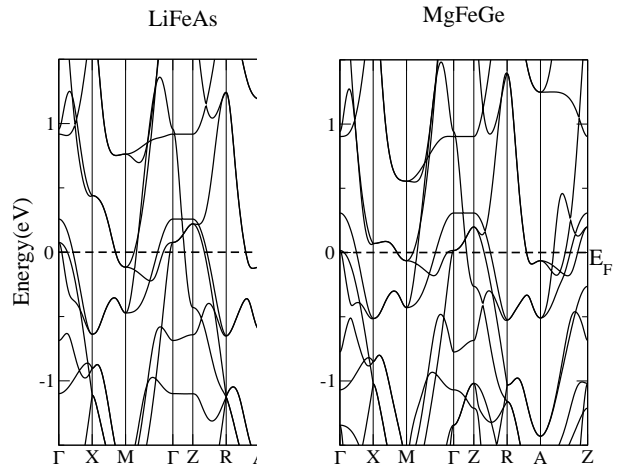


FIG. 4: (Color online) Band structures of LiFeAs and MgFeGe near the Fermi energy. The differences at Γ , M, and X are discussed in the text.

LiFeAs					
$m \backslash m'$	-2	-1	0	+1	+2
-2	0.646	0.000	0.000	0.000	-0.033
-1	0.000	0.626	0.000	0.000	0.000
0	0.000	0.000	0.698	0.000	0.000
+1	0.000	0.000	0.000	0.616	0.000
+2	-0.033	0.000	0.000	0.000	0.625

MgFeGe					
$m \backslash m'$	-2	-1	0	+1	+2
-2	0.645	0.000	0.000	0.000	-0.038
-1	0.000	0.635	0.000	0.000	0.000
0	0.000	0.000	0.683	0.000	0.000
+1	0.000	0.000	0.000	0.623	0.000
+2	-0.038	0.000	0.000	0.000	0.621

TABLE II: Fe 3d orbital occupation matrix elements $n_{mm'}$ of LiFeAs and MgFeGe, from the LAPW sphere of radius $R = 2.47$ a.u.

than hybrid or GW calculations,²⁵ in which the gap corrections are comparable in accuracy.

The mBJ potential has not however been tested on many metals or semimetals. Singh⁴³ studied LaFeAsO using the mBJ potential and concluded that while the 10% smaller bandwidth agreed better with experiment than without mBJ, the slight changes in the FSs were within the margins of uncertainty when one compares an experimental to a relaxed As position. One can note that LaFeAsO and the two compounds we study here are semimetals (*i.e.*, “insulators” with slightly overlapping valence and conduction bands²⁶) so a functional that

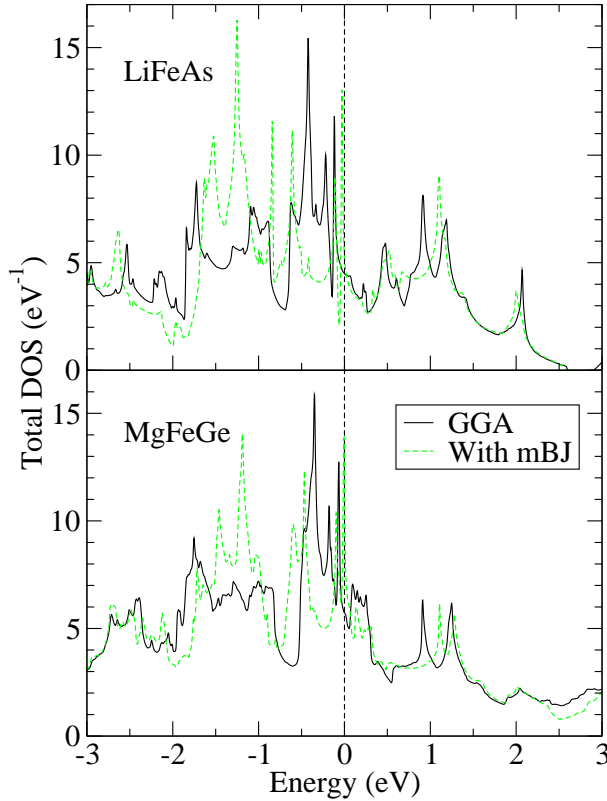


FIG. 5: (Color online) Total DOS comparisons between the non-mBJ (regular GGA) and mBJ calculations of LiFeAs (above) and MgFeGe (below).

makes favorable corrections for insulators might lead to similar improvements for semimetals.

A. Bands and DOS

The DOS spectra of LiFeAs and MgFeGe from calculations with and without the use of mBJ are compared in Fig. 5, where it can be seen that the position and intensity of peaks is altered in many energy regions. In LiFeAs, the distribution of Fe weight is influenced strongly by the mBJ potential in the range of -2.5 eV to 1 eV, due to the restructuring of some bands, shown in Fig. 6. Applying the mBJ potential, the bands that make the electron pockets surrounding the zone corners move up to create a van Hove singularity at ε_F . Angle-resolved photoemission spectra (ARPES) of LiFeAs reveal a van Hove singularity at the Fermi energy;¹³ this is however not born out of the zone-corner electron FSs, as is the case in our mBJ calculation, but rather the two smaller hole FSs centered at Γ (see Fig. 7). According to ARPES measurements, these particular

FSs are quite a bit smaller than those derived from a DFT calculation. The flat band at 0.25 eV along the Γ -Z line maintains its flatness but is shifted to slightly below the Fermi energy. This is the same band that crosses the FS to create the largest hole pocket at Γ , so its shifting below ε_F results in the hole FS disappearing. The two (originally) smaller hole enclosures increase in size while the electron pockets overall become smaller under the mBJ potential (see also Fig. 7 for the pre- and post-mBJ FSs of LiFeAs).

The same trends can be observed in MgFeGe. Changes due to the mBJ potential occur between -2 eV and 1.2 eV, including the formation of a van Hove singularity at the Fermi level, again caused by the increase in states at ε_F due to the shrinking electron FSs, shown in Fig. 8. The largest hole pocket is significantly reduced in size and the smaller two are enlarged. The electron pockets take on a peculiar shape in which the “waist” is squeezed such that the M point is no longer enclosed by the FSs.

B. Orbital selectivity of the differences

There is intense interest in the multi-orbital nature of the iron-pnictides and specifically how much each one contributes near the Fermi level. There is also a need to understand in more detail orbital-dependent effects due to the TB-mBJ exchange potential. Figs. 9 and 10 dissect the DOSs of LiFeAs and MgFeGe respectively, into Fe d orbital projected densities of states (PDOS). Our GGA results are consistent with those of Nekrasov and collaborators.³² The t_{2g} orbitals dominate the Fermi level for any exchange-correlation functional for both systems. Using mBJ, (i) the d_{z^2} and d_{xy} states shift downward by ~ 0.5 eV, whereas the $d_{x^2-y^2}$ move upward by a similar amount; (ii) the $d_{xz/yz}$ occupied bandwidth narrows and the peak near ε_F moves to the Fermi level. Note that it is these $d_{xz/yz}$ orbitals that are responsible for the sharp peak structure near or at ε_F . As for the differences between materials, the shift of the d_{xy} states is larger for LiFeAs, whose substantial d_{xy} -orbital PDOS at ε_F drops as a result by an order of magnitude, from 0.75 eV $^{-1}$ to 0.07 eV $^{-1}$. The $d_{xz/yz}$ van Hove singularity makes the value of $N(\varepsilon_F)$ very sensitive to details (in exchange-correlation potential, probably to structure, etc.).

Borisenko *et al.*¹³ noted that the smaller Γ -centered hole FSs of LiFeAs derived from DFT are not realistic, their being much smaller than observed in ARPES data. Two separate studies, by Yin *et al.*⁴⁴ and Ferber *et al.*,⁴⁵ have shown that using DFT+DMFT improves on the DFT band structure,

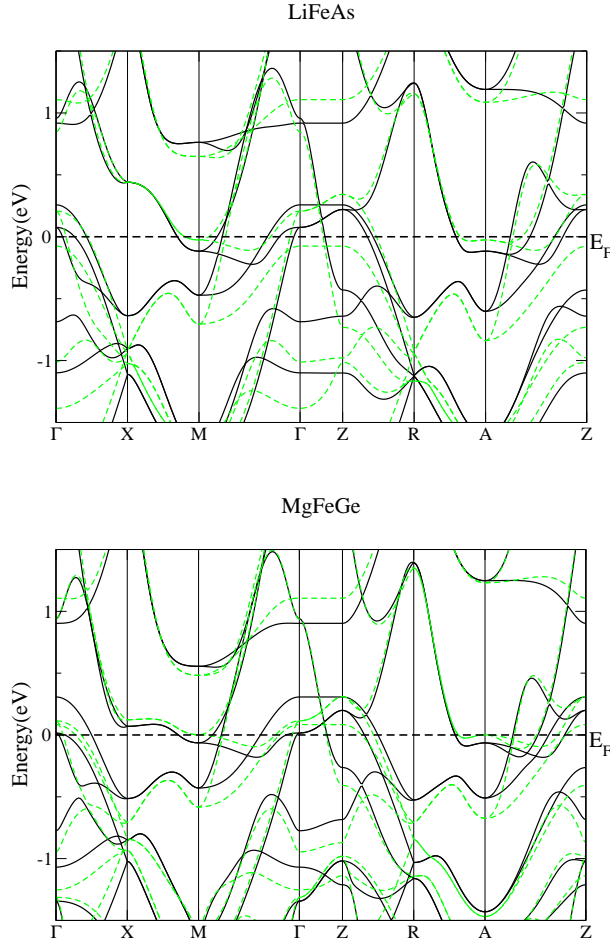


FIG. 6: (Color online) Band structures of LiFeAs and MgFeGe without (solid, black) and with (dashed, green) mBJ implementation.

yielding FSs more consistent with experiment: the outer pocket at Γ is larger and the inner pockets are much smaller. Looking at Fig. 7, it may at first glance seem as if the mBJ potential affects the three hole pockets in the same way DMFT affects them. But, as mentioned before, upon observation of the bands crossing the Fermi energy along Γ -X and Z-R, it is evident that quite the opposite happens: the largest pocket disappears below the Fermi energy and the two smaller pockets become larger. The mBJ potential acts upon the MgFeGe system in a similar fashion. It decreases the sizes of the outer hole cylinder and the two electron pockets, and increases the size of the smallest hole pocket. Overall, the mBJ-applied calculation generates less two-dimensional FSs, and does not improve agreement with experiment.

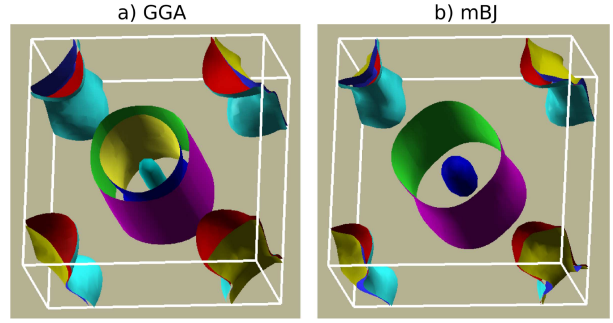


FIG. 7: (Color online) FSs in the Brillouin zone, from a) a non-mBJ and b) an mBJ calculation of LiFeAs. Γ is located at the unit center.

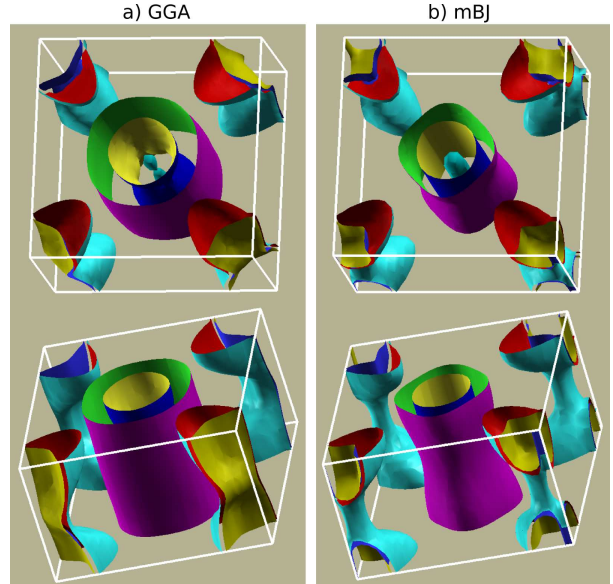


FIG. 8: (Color online) FSs in the Brillouin zone, from a) a non-mBJ and b) an mBJ calculation of MgFeGe. Γ is located at the unit center.

C. Changes in orbital occupancies

In both cases of LiFeAs and MgFeGe, when the mBJ potential is added, the charge surrounding the Fe atom becomes more anisotropic, concentrating more in the direction of the As/Ge atom. Despite the visible change in the density contours (not shown here) upon application of mBJ, the total 3d occupation within the MT sphere of LiFeAs remains unchanged (6.65 for our sphere radius), and that of MgFeGe decreases almost imperceptibly (6.64 to 6.63). Thus there is only a redistribution between 3d orbitals. Indeed, as shown in Table III the d_{z^2} occupation increases whereas that of $d_{xz/yz}$ decreases,

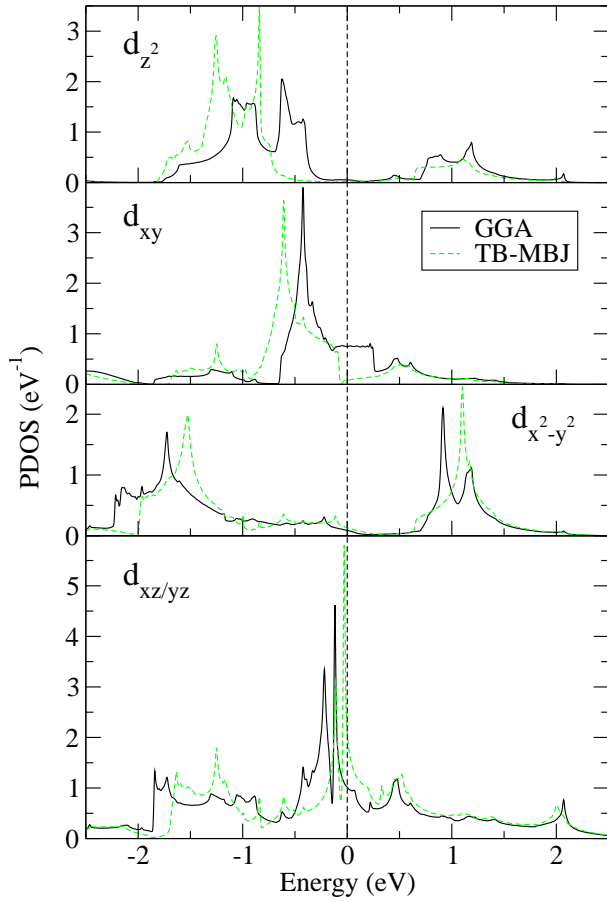


FIG. 9: (Color online) Fe partial DOSs of LiFeAs with and without TB-mBJ.

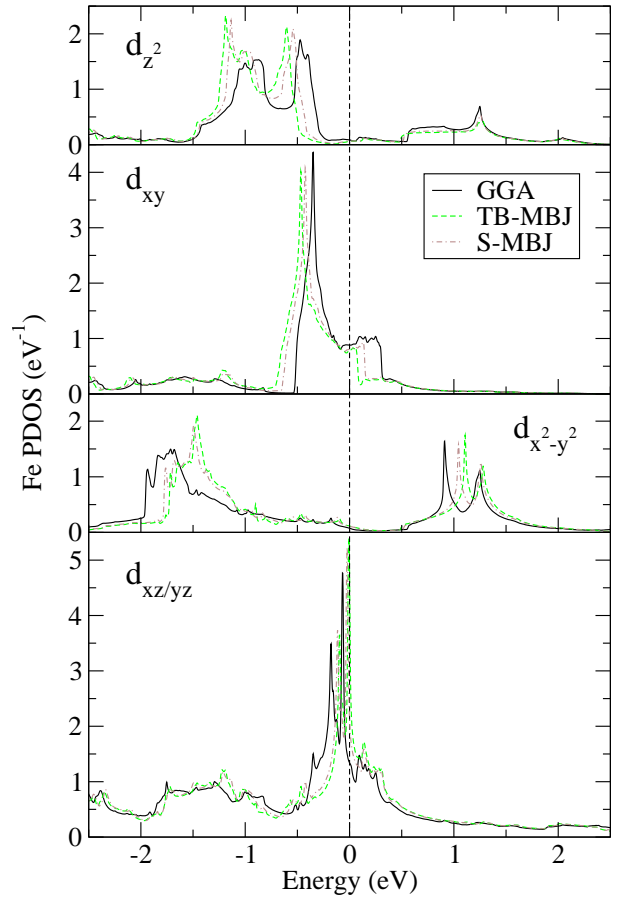


FIG. 10: (Color online) Fe PDOSs of MgFeGe without mBJ, with TB-mBJ, and with S-mBJ.

by 7-10% for both compounds.

While the mBJ formalism is not intrinsically specific to gapped materials, the parametrizing of the coefficients is done empirically by using insulators and semiconductors to match the bandgap. Tran and Blaha's justification for using orbitally independent potentials to obtain orbitally *dependent* bandgaps is that gapped systems typically have a small overlap between the occupied and unoccupied orbitals. This is not the case for metals, however, and the mBJ implementation may give bogus results if the unoccupied orbital potentials are characteristically different from the occupied.

IV. SUMMARY

In this study we have made a comparison of several aspects of the electronic structures of LiFeAs and isoelectronic MgFeGe. A repositioning of a DOS peak a few tenths of an electron-volt above the Fermi

level is the most obvious difference, likely arising due to differences in Fe hybridization with Ge compared to As. As noted in the original report,²² the band structures near the Fermi level are very similar. We have further established that the Fe total 3d orbital occupations for the Fe atom are identical for the two compounds, and individual orbital occupations differ by very little—interesting but too little to be significant. The As-Fe-As and Ge-Fe-Ge angles, although far from being tetrahedrally regular as is the case in the higher T_c FeSCs, do not differ significantly in these two compounds. The band structures are in fact more similar than in other FeSCs that show larger variation but comparable superconducting properties. MgFeGe's higher density of states at the Fermi energy is significant, but argues that MgFeGe should be the *better* superconductor, rather than being nonsuperconducting.

We have tested the recently extended TB-mBJ exchange potential for these compounds, since it is an exchange potential that seems to work well

LiFeAs					
$m \backslash m'$	-2	-1	0	+1	+2
-2	0.683	0.000	0.000	0.000	-0.109
-1	0.000	0.565	0.000	0.000	0.000
0	0.000	0.000	0.763	0.000	0.000
+1	0.000	0.000	0.000	0.554	0.000
+2	-0.109	0.000	0.000	0.000	0.665

MgFeGe					
$m \backslash m'$	-2	-1	0	+1	+2
-2	0.677	0.000	0.000	0.000	-0.106
-1	0.000	0.590	0.000	0.000	0.000
0	0.000	0.000	0.734	0.000	0.000
+1	0.000	0.000	0.000	0.576	0.000
+2	-0.106	0.000	0.000	0.000	0.658

TABLE III: Fe 3*d* density occupation matrix elements $n_{mm'}$ of LiFeAs and MgFeGe under the TB-mBJ potential.

for non-magnetic insulators. The differences have been quantified, but do not seem to resolve the conflict with experimental (ARPES) observations. Thus exchange effects between occupied and unoccupied non-magnetic states seem to be treated well with TB-mBJ, whereas magnetic fluctuations, which are also exchange in origin and are treated rather well within DFT+DMFT, are not treated well by the TB-mBJ approach.

Our results have not revealed any clearly essential features that leave MgFeGe nonsuperconducting while LiFeAs is an impressive, if not yet well understood, superconductor with a relatively high T_c . We suggest that further exploration in parallel of these two compounds, by experiment and theoretically, will provide one of the most promising approaches to identifying the superconducting mechanism in LiFeAs and, possibly, in the full class of FeSCs.

V. ACKNOWLEDGMENTS

We thank Y. Quan for emphasizing the importance of the radial density in characterizing the 3*d*

occupation in transition metal compounds. This work was supported by a DOE Computational Materials and Chemical Science Network grant de-sc0005468.

VI. APPENDIX: COMMENTS ON THE TB-MBJ POTENTIAL

Recently, improvements on the original mBJ potential (TB-mBJ) have been made to refit and create new sets of parameters based on the type of solid (semiconductor, ionic insulator, noble-gas solid, etc.) and also by incorporating more gapped systems.⁴⁶ As LiFeAs and MgFeGe are, of these types, closest in character to semiconductors, we adopted the semiconductor parameters and applied this new potential, referred to as the S-mBJ potential, to the DFT GGA calculations on our compounds. The difference between the LiFeAs calculations using TB-mBJ and S-mBJ is negligible and hence not shown here, but it is more noticeable in MgFeGe. Upon observation of the PDOSs of Fe in MgFeGe in Fig. 10, it is apparent that the S-mBJ system is an intermediary of the non-mBJ and TB-mBJ systems. This makes sense since the parameters of the TB-mBJ potential were determined using larger-gapped materials as well.

Implementing the mBJ potential on LiFeAs/MgFeGe increases the occupations of Fe and As/Ge but decreases the Li/Mg occupation. While the TB-mBJ and S-mBJ methods result in very similar band structures for LiFeAs, in the case of MgFeGe, more noticeable shifts in energy of the electronic states can be observed. The parameter c in Eq. 7 of Ref. 46 is determined by the fitted parameters A and B (for S-mBJ, $A = 0.267$ and $B = 0.656$), as well as the averaged gradient of the density, \bar{g} , which differs from system to system. For LiFeAs $\bar{g} = 1.39$ a.u.⁻¹, and for MgFeGe $\bar{g} = 1.27$ a.u.⁻¹. As \bar{g} deviates further from ~ 1.4 a.u.⁻¹, so does c_{semi} from c_{TB} . In the case of LiFeAs, $c_{\text{semi}} \approx c_{\text{TB}}$, but this is not true of MgFeGe.

¹ Y. Fuseya, T. Kariyado, and M. Ogata, J. Phys. Soc. Jpn. **78**, 023703 (2009).

² H. Zhai, F. Wang, and D.-H. Lee, Phys. Rev. B **80**, 064517 (2009).

³ T. A. Maier, S. Graser, P. J. Hirschfeld, and D. J.

Scalapino, Phys. Rev. B **83**, 100515 (2011).

⁴ C. Fang, Y.-L. Wu, R. Thomale, B. A. Bernevig, and J. Hu, Phys. Rev. X **1**, 011009 (2011).

⁵ P. M. R. Brydon, M. Daghofer, C. Timm, and J. van den Brink, Phys. Rev. B **83**, 060501 (2011).

- ⁶ T. Saito, S. Onari, and H. Kontani, *Phys. Rev. B* **82**, 144510 (2010).
- ⁷ S. Zhou, G. Kotliar, and Z. Wang, *Phys. Rev. B* **84**, 140505 (2011).
- ⁸ M. Berciu, I. Elfimov, and G. A. Sawatzky, *Phys. Rev. B* **79**, 214507 (2009).
- ⁹ H. Takahashi, Y. Imai, S. Komiyama, I. Tsukada, and A. Maeda, *Phys. Rev. B* **84**, 132503 (2011).
- ¹⁰ L. Boeri, O. V. Dolgov, and A. A. Golubov, *Phys. Rev. Lett.* **101**, 026403 (2008).
- ¹¹ T. Egami, B. Fine, D. Parshall, A. Subedi, and D. Singh, *Adv. Condens. Matt. Phys.* **2010**, 164916 (2010).
- ¹² Y. Kamihara, T. Watanabi, M. Hirano, and H. Hosono, *J. Am. Chem. Soc.* **130**, 3296 (2008).
- ¹³ S. V. Borisenko, V. B. Zabolotnyy, D. V. Evtushinsky, T. K. Kim, I. V. Morozov, A. N. Yaresko, A. A. Kordyuk, G. Behr, A. Vasiliev, R. Follath, et al., *Phys. Rev. Lett.* **105**, 067002 (2010).
- ¹⁴ K. Kusakabe and A. Nakanishi, *J. Phys. Soc. Jpn.* **78**, 124712 (2009).
- ¹⁵ S. Deng, J. Köhler, and A. Simon, *Phys. Rev. B* **80**, 214508 (2009).
- ¹⁶ C. He, Y. Zhang, B. P. Xie, X. F. Wang, L. X. Yang, B. Zhou, F. Chen, M. Arita, K. Shimada, H. Namatame, et al., *Phys. Rev. Lett.* **105**, 117002 (2010).
- ¹⁷ L. Ma, G. F. Chen, D.-X. Yao, J. Zhang, S. Zhang, T.-L. Xia, and W. Yu, *Phys. Rev. B* **83**, 132501 (2011).
- ¹⁸ K. Kitagawa, Y. Mezaki, K. Matsubayashi, Y. Uwatoko, and M. Takigawa, *J. Phys. Soc. Jpn.* **80**, 033705 (2011).
- ¹⁹ D. R. Parker, M. J. Pitcher, P. J. Baker, I. Franke, T. Lancaster, S. J. Blundell, and S. J. Clarke, *Chem. Commun.* pp. 2189–2191 (2009).
- ²⁰ C. Chu, F. Chen, M. Gooch, A. Guloy, B. Lorenz, B. Lv, K. Sasmal, Z. Tang, J. Tapp, and Y. Xue, *Physica C* **469**, 326 (2009).
- ²¹ I. Morozov, A. Boltalin, O. Volkova, A. Vasiliev, O. Kataeva, U. Stockert, M. Abdel-Hafiez, D. Bombor, A. Bachmann, L. Harnagea, et al., *Cryst. Growth Des.* **10**, 4428 (2010).
- ²² X. Liu, S. Matsuishi, S. Fujitsu, and H. Hosono, *Phys. Rev. B* **85**, 104403 (2012).
- ²³ C.-H. Lee, A. Iyo, H. Eisaki, H. Kito, M. T. Fernandez-Diaz, T. Ito, K. Kihou, H. Matsuhata, M. Braden, and K. Yamada, *J. Phys. Soc. Jpn.* **77**, 083704 (2008).
- ²⁴ D. Johrendt, H. Hosono, R.-D. Hoffmann, and R. Pöttgen, *Z. Kristallogr.* **226**, 435 (2011).
- ²⁵ F. Tran and P. Blaha, *Phys. Rev. Lett.* **102**, 226401 (2009).
- ²⁶ S. Lebègue, Z. P. Yin, and W. E. Pickett, *New J. Phys.* **11**, 025004 (2009).
- ²⁷ P. Blaha, K. Schwarz, P. Sorantin, and S. Trickey, *Comp. Phys. Comm.* **59**, 399 (1990).
- ²⁸ K. Schwarz and P. Blaha, *Comput. Mater. Sci.* **28**, 259 (2003).
- ²⁹ J. P. Perdew, K. Burke, and M. Ernzerhof, *Phys. Rev. Lett.* **77**, 3865 (1996).
- ³⁰ J. H. Tapp, Z. Tang, B. Lv, K. Sasmal, B. Lorenz, P. C. W. Chu, and A. M. Guloy, *Phys. Rev. B* **78**, 060505 (2008).
- ³¹ D. J. Singh, *Phys. Rev. B* **78**, 094511 (2008).
- ³² I. Nekrasov, Z. Pchelkina, and M. Sadovskii, **88**, 543 (2008).
- ³³ M. Wang, M. Wang, H. Miao, S. V. Carr, D. L. Abernathy, M. B. Stone, X. C. Wang, L. Xing, C. Q. Jin, X. Zhang, et al., *ArXiv e-prints* (2012), 1208.0909.
- ³⁴ G. A. Sawatzky, I. S. Elfimov, J. van den Brink, and J. Zaanen, *Europhys. Lett.* **86**, 17006 (2009).
- ³⁵ G. Lee, H. S. Ji, Y. Kim, C. Kim, K. Haule, G. Kotliar, B. Lee, S. Khim, K. H. Kim, K. S. Kim, et al., *ArXiv e-prints* (2012), 1205.6526.
- ³⁶ P. Jeglič, A. Potočnik, M. Klanjšek, M. Bobnar, M. Jagodič, K. Koch, H. Rosner, S. Margadonna, B. Lv, A. M. Guloy, et al., *Phys. Rev. B* **81**, 140511 (2010).
- ³⁷ Z. Li, Y. Ooe, X.-C. Wang, Q.-Q. Liu, C.-Q. Jin, M. Ichioka, and G. Qing Zheng, *J. Phys. Soc. Jpn.* **79**, 083702 (2010).
- ³⁸ L. Ma, J. Zhang, G. F. Chen, and W. Yu, *Phys. Rev. B* **82**, 180501 (2010).
- ³⁹ A. E. Taylor, M. J. Pitcher, R. A. Ewings, T. G. Per-ring, S. J. Clarke, and A. T. Boothroyd, *Phys. Rev. B* **83**, 220514 (2011).
- ⁴⁰ A. D. Becke and E. R. Johnson, *J. Chem. Phys.* **124**, 221101 (2006).
- ⁴¹ R. T. Sharp and G. K. Horton, *Phys. Rev.* **90**, 317 (1953).
- ⁴² J. D. Talman and W. F. Shadwick, *Phys. Rev. A* **14**, 36 (1976).
- ⁴³ D. J. Singh, *Phys. Rev. B* **82**, 205102 (2010).
- ⁴⁴ Z. Yin, K. Haule, and G. Kotliar, *Nature Mater.* **10**, 932 (2011).
- ⁴⁵ J. Ferber, K. Foyevtsova, R. Valentí, and H. O. Jeschke, *Phys. Rev. B* **85**, 094505 (2012).
- ⁴⁶ D. Koller, F. Tran, and P. Blaha, *Phys. Rev. B* **85**, 155109 (2012).